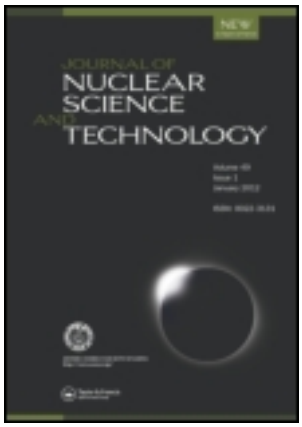

Journal of Nuclear Science and Technology
Publication details, including instructions for authors and subscription information:
http://www.tandfonline.com/loi/tnst20

New Spacer Grid to Enhance Mechanical/Structural Performance

Kee Nam Song [a] , Soo Bum Lee [b] , Moon Kyun SHIN [c] , Jae Jun LEE [c] & Gyung Jin PARK [c]
[a] Korea Atomic Energy Research Institute , P.O. Box 105, Yusong, Daejeon , 305-600 , Republic of Korea
[b] 1174 Engineering Lab. , University of Maryland , College Park , MD , 20742 , USA
[c] Division of Mechanical and Information Management Engineering , Hanyang University , Sa 3-dong, Sangnok-gu, Ansan City, Gyeonggi-do , 426-791 , Republic of Korea
Published online: 05 Jan 2012.

To cite this article: Kee Nam Song , Soo Bum Lee , Moon Kyun SHIN , Jae Jun LEE & Gyung Jin PARK (2010) New Spacer Grid to Enhance Mechanical/Structural Performance, Journal of Nuclear Science and Technology, 47:3, 295-303

To link to this article: http://dx.doi.org/10.1080/18811248.2010.9711957

Journal of NUCLEAR SCIENCE and TECHNOLOGY, Vol. 47, No. 3, p. 295–303 (2010)

ARTICLE

New Spacer Grid to Enhance Mechanical/Structural Performance

Kee Nam SONG[1,*], Soo Bum LEE[2,†], Moon Kyun SHIN[3], Jae Jun LEE[3] and Gyung Jin PARK[3]

[1]*Korea Atomic Energy Research Institute, P.O. Box 105, Yusong, Daejeon 305-600, Republic of Korea*
[2]*1174 Engineering Lab., University of Maryland, College Park, MD20742, USA*
[3]*Division of Mechanical and Information Management Engineering, Hanyang University, Sa 3-dong, Sangnok-gu, Ansan City, Gyeonggi-do 426-791, Republic of Korea*

(Received September 7, 2009 and accepted in revised form November 20, 2009)

A spacer grid (SG), which supports nuclear fuel rods (FRs) laterally and vertically with a friction grip, is one of the most important structural components in a PWR fuel. The forms of the grid straps and spring form are known to be closely related with the SG crush strength and the integrity of FR support, respectively. In this study, a new SG form and its manufacturing technology were suggested for enhancing the integrity of the FR support and the SG crush strength by using a systematic optimization technique without significantly increasing the pressure drop across the reactor core. Finite element (FE) analysis and crush strength tests on the new SG form were carried out to check the performance enhancement compared with commercial SGs. According to the results, it is estimated that the actual critical load enhancement of the SG is approximately up to 30%, and the actual contact area, when an FR is inserted into an SG cell, is more than double for the new SG form. And also, some design variables that affect the SG crush strength were classified and their effects on the crush strength were investigated by an FE analysis and a crush strength test.

KEYWORDS: spacer grid, pwr, fuel rod integrity, nuclear fuel assembly, crush strength, fretting wear, dimple, spring, optimization, axiomatic design

I. Introduction

A fuel assembly in a Pressurized light Water Reactor (PWR) consists of spacer grids, fuel rods, a top nozzle, one bottom nozzle, guide tubes, and an instrumentation tube as shown in **Fig. 1**. Among them, the spacer grid assembly is an interconnected array of slotted grid straps, welded at the intersections to form an egg crate structure. The spacer grid assembly supports the fuel rod with springs and dimples stamped into each grid strap within a spacer grid cell, as shown in **Fig. 2**. And also, the spacer grid protects the fuel rods from external impact loads in an abnormal operating environment such as during an earthquake or a Loss-Of-Coolant Accident (LOCA). Moreover, the spacer grid assembly must keep the instrumentation tube straight so that a plant's neutronic instrumentation can be inserted freely and removed from the tube even after the lateral loading conditions have been exceeded. Therefore, the plastic deformation of a spacer grid assembly needs to be designed to have enough lateral impact strength.[1)]

Several studies have been devoted to the experiments, analyses, and design of a spacer grid.[2–7)] The design and material for a spacer grid and design optimization of the outer plate in a spacer grid have been performed by considering the stiffness, impact strength, and flow restriction.[2,3)] The buckling behavior is one of the important performances to evaluate the lateral strength because the deformation of spacers needs to be limited to safely maintain the guide thimbles under an abnormal operating condition such as during an earthquake.[4,5)] A finite element (FE) method for predicting the buckling behavior of a spacer grid structure has been established,[6–8)] reflecting a real test environment, using a commercial FE code ABAQUS/Explicit. An effort to improve the buckling resistance of a support grid using an axiomatic design and optimization skills has been reported,[9,10)] where the dimple location and welding penetration depth at the intersection of the grid have been studied and optimized.

II. Enhancement of a Fuel Rod Support

Mostly, structural design is performed in order to maximize structural performance while constraints are satisfied. The constraints are usually imposed on the deformations or stresses. In some problems, we may have a constraint to maintain a specific geometric shape of a structure. Such constraints exist in the designs of the satellite antenna, the main reflector of a large telescope, the truss structure that must maintain a certain geometric shape like a quadratic equation, and the smart structure that generates specific response values.[11,12)]

*Corresponding author, E-mail: knsong@kaeri.re.kr
†Present address: *Korea Atomic Energy Research Institute, P.O.Box 105, Yusong, Daejeon 305-600, Republic of Korea*

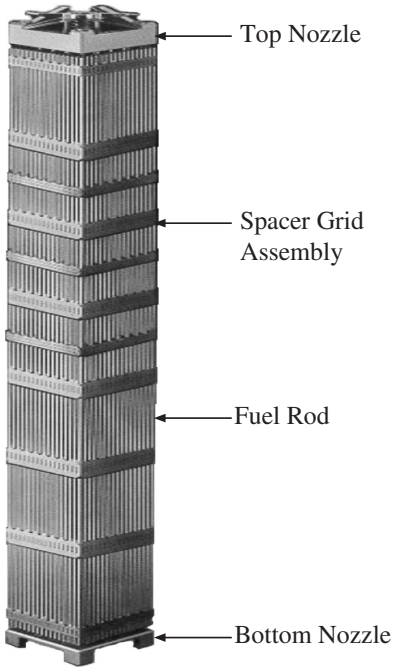

Fig. 1 PWR fuel assembly

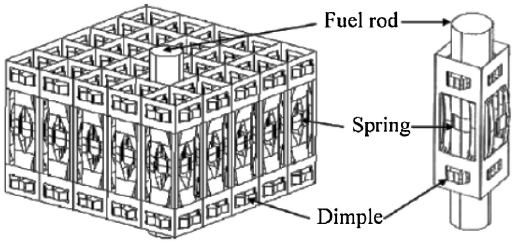

a) Spacer grid and unit cell

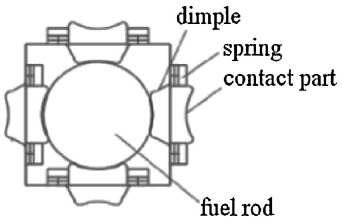

b) Cross section of unit cell

Fig. 2 Spacer grid and cross section of spacer grid unit cell

1. Homology Design

The homology deformation defined by Hoerner[13] is to be maintained to have a certain geometric shape of the structure with a given number of structural points before, during, and after the deformation. Homology design is a design method that maintains a given geometrical shape based on the homology deformation. In other words, designers predict the deformation or the natural frequency of the entire structure or a part. In the homology design, design variables are determined to have the predicted response values.[2,12,14] In the optimization of the spacer grid spring, homology deformation, which holds a certain shape after the deformation, is utilized.

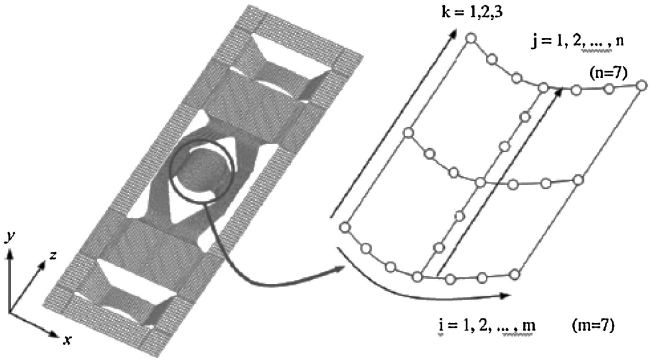

Fig. 3 Choice of nodes for homology constraint

2. Conditions to Enhance the Fuel Rod Support

It is well known that the shape of the spring has a great influence on the fuel rod fretting wear from experiments.[2,15,16] In order to minimize the fretting wear, the spacer grid should be designed to have a large contact area between the spring and the fuel rod.[17] From the viewpoint of homology design, the deformed shape of the spring should be the same as that of the fuel rod. If the contact area is larger, the surface pressure will be reduced, and the fretting wear will be reduced.

Two conditions for reducing the fretting wear are proposed.[10,18,19] First, the fuel rod and the spring should have the same curvature in the section of the fuel rod. Thus, the design is formulated to minimize the difference between the two curvatures. Second, the shape of the spring center should be straight in the direction of the fuel rod. These conditions are imposed as constraints of the optimization process.

3. Formulation for Optimization

In order to enhance the resistance of fretting wear and the stable support of the fuel rod, the contact area between a spacer grid spring and a fuel rod should be enlarged when the fuel rod is inserted in the spacer grid cell, and this condition means that the deformed shape of the spring should be the same as that of the fuel rod. The deformation of the fuel rod is negligible; therefore, the fuel rod is assumed to be rigid. This condition is defined as a homology constraint and used in the optimization process.

The objective function is defined by using the homology conditions. The shape of the spacer grid spring is presented in **Fig. 3**. Homology constraints are defined on the x-y plane and the y-z plane in Fig. 3. The objective function is defined with several nodes because the objective function cannot be defined with all the nodes of the contact area in the spring. The objective function on the x-y plane is the minimized difference between the curvatures of the fuel rod and the deformed spring.

As illustrated in **Fig. 4**, seven nodes are selected for the objective function on the x-y plane. The objective function on the x-y plane is as follows:

$$\sum_{j=1}^{7}(R - L'_j)^2, \tag{1}$$

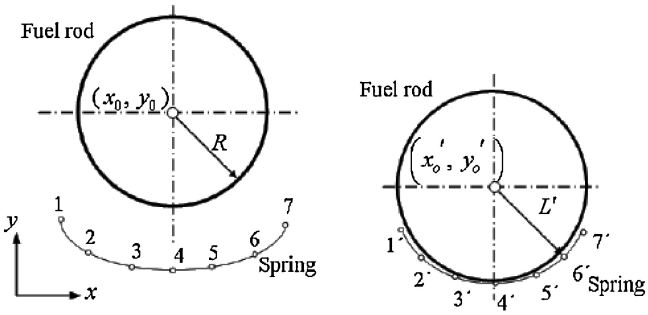

(a) Before deformation (b) After deformation

Fig. 4 Contact between the spring and the fuel rod (radial)

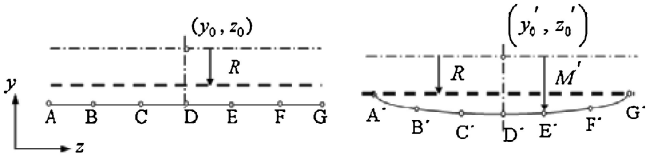

(a) Before deformation (b) After deformation

Fig. 5 Contact between the spring and the fuel rod (axial)

where R is the radius of the fuel rod and L' is the distance from the selected nodes of the spring to the center of the fuel rod after deformation. Three nodes are selected in the z direction in the same way. The objective function in the z direction is as follows:

$$\sum_{k=1}^{3}\sum_{i=1}^{7}(R - L'_{ik})^2. \tag{2}$$

The objective function on the y-z plane is that the deformed shape of the spring center should be straight. As illustrated in **Fig. 5**, seven nodes are selected for the objective function. This objective function is as follows:

$$\sum_{j=1}^{7}(R - M'_j)^2, \tag{3}$$

where M' is the distance from the deformed spring center to the selected nodes. The difference between M' and the radius of the fuel rod should be minimized in Eq. (3).

The final objective function used for optimization is a multiobjective function of each plane by the weighting factor. This objective function is as follows:

$$(1-a)\sum_{k=1}^{3}\sum_{i=1}^{7}(R - L'_{ik})^2 + \sum_{j=1}^{7}(R - M'_j)^2. \tag{4}$$

Equation (4) is a homology equation. Constraints for optimization are defined. First, the weight of the spacer grid (w) should not be larger than that of the initial model (w_{initial}). Second, due to the radiation by neutron in the reactor, only 8% of the initial spring force remains after long-term operation. A load of about 2 N from the fluid-induced vibration and a load of about 1.2 N from the transport of nuclear fuel assembly are applied to the spring. Therefore, the initial spring force must be greater than 40 N to support the fuel rod throughout the operating period.[20)]

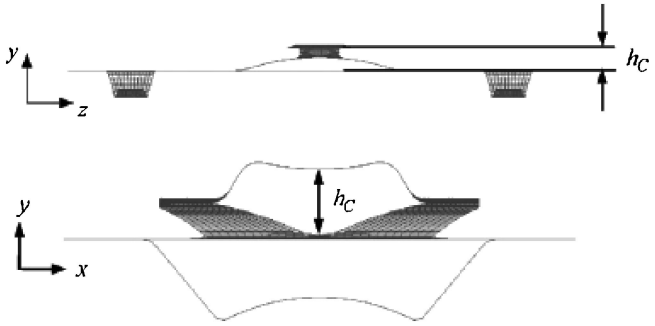

Fig. 6 Height of spring center

As mentioned earlier, the spring force is the reaction force at the edges of the spacer grid. Third, the height of the spring center (h_c) before deformation must be larger than 1.65 mm. This is shown in **Fig. 6**. If the height of the spring center is smaller than 1.65 mm, then the spring force is smaller than 40 N in nonlinear static analysis after optimization. It is formed from numerical experiment. Finally, the stress of the spacer grid (σ) is smaller than the allowable stress of the spacer grid ($\sigma_{\text{allowable}}$), such as the yield stress of the spacer grid material.

$$\begin{aligned}
&\text{Find} && b_n \quad n = 1, \cdots, 29\\
&\text{to minimize} && (1-\alpha)\sum_{k=1}^{3}\sum_{i=1}^{7}(R - L'_{ik})^2 + \sum_{j=1}^{7}(R - M'_j)^2\\
&\text{subject to} && w \le w_{\text{initial}}\\
&&& F_{\text{spring}} \ge 40\,\text{N}\\
&&& h_c \ge 1.65\,\text{mm}\\
&&& \sigma \le \sigma_{\text{allowable}}
\end{aligned} \tag{5}$$

Equation (5) is the formulation for optimization. However, this formulation cannot include the plastic deformation. Therefore, it is necessary to convert the formulation so as to permit the plastic deformation and to reduce the maximum stress. This formulation is converted to a min-max problem. When a maximum property is included in the optimization formulation, the problem can be solved by using the Taylor-Benson 'beta' formulation as follows:

$$\begin{aligned}
&\text{Find} && b_n && n = 1, \cdots, 29\\
&\text{to minimize} && \beta\\
&\text{subject to} && w \le w_{\text{initial}}\\
&&& F_{\text{spring}} \ge 40\,\text{N}\\
&&& h_c \ge 1.65\,\text{mm}\\
&&& (R - L'_{ik})^2 \le C_h && i = 1, \cdots, 7; k = 1, 2, 3\\
&&& (R - M'_j)^2 \le C_h && j = 1, \cdots, 7\\
&&& \sigma \le \beta,
\end{aligned} \tag{6}$$

where β is the artificial variable used for the objective function of a min-max problem; new constraints (C_h) are defined on each plane. Thus, the artificial variable β is minimized while the constraints including all the stresses are satisfied. It is noted that Eq. (6) does not have a constraint for allowable stress so that plastic deformation is allowed. The homology constraints, which must be smaller than a homology constant (C_h), are defined on each plane. The homology constant should be appropriately defined.

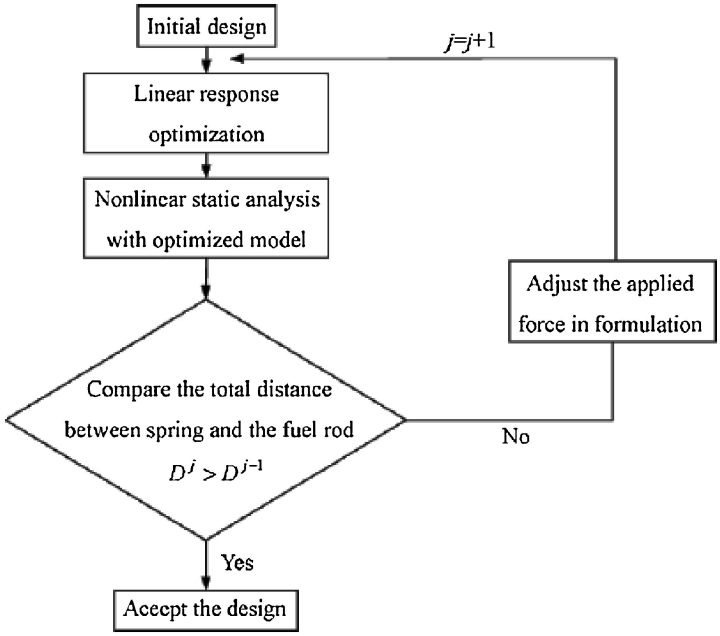

Fig. 7 Flow chart of optimization for a spacer grid spring

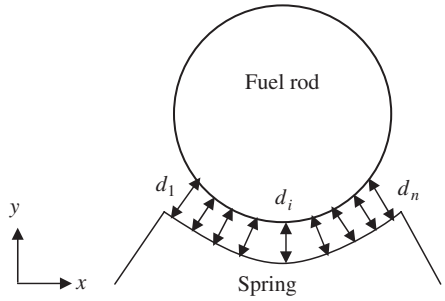

Fig. 8 Definition of the total distance

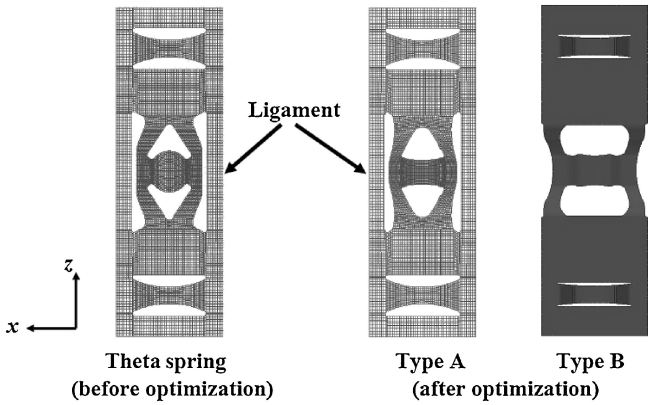

Fig. 9 Spring shape before and after optimization

4. Flow Chart for Optimization

A design process is defined as illustrated in **Fig. 7**. It is extremely difficult to directly consider nonlinear analysis in structural optimization. It is desirable to exploit the benefit of linear static optimization. First, linear response optimization is performed with the initial model. To verify the optimization process, nonlinear static analysis is performed with the optimized model. If the analysis results satisfy the convergence criteria, the optimization process is terminated. Otherwise, as mentioned earlier, new loads are calculated with the results of nonlinear static analysis, and optimization is performed again by using the new loads until the convergence criterion is satisfied. The convergence criterion is defined using the total distance, which is the sum of the distances between all the nodes of the fuel rod and that of the contact part of the spacer grid spring. The distances are illustrated in **Fig. 8**, and the total is calculated as

$$D^j = \sum_{i=1}^{n} d_i. \tag{7}$$

If the total distance of the current cycle is larger than that of the previous cycle, the optimization process is terminated.

5. Results of Enhancement

The spacer grid spring shapes are shown in **Fig. 9** before and after optimization. Two kinds of optimization are obtained for cases such as when there are ligaments (Type A) or not (Type B) near the spring, as shown in Fig. 9. The enhancement of fuel rod support was confirmed by comparisons of the contact area, peak stresses, and plastic deformation of a spacer grid spring when inserting a fuel rod into a spacer grid structure. The normalized enhancement of a fuel rod support is shown in **Table 1**. According to Table 1, a considerable enhancement of a fuel rod support is achieved

GENESIS 7.5[21] is used for optimization of the spacer grid spring, and the modified method of feasible direction (MMFD) algorithm is utilized in order to enhance the resistance of fretting wear and the stable support of the fuel rod; the contact area between a spacer grid spring and a fuel rod should be enlarged when the fuel rod is inserted in the spacer grid.

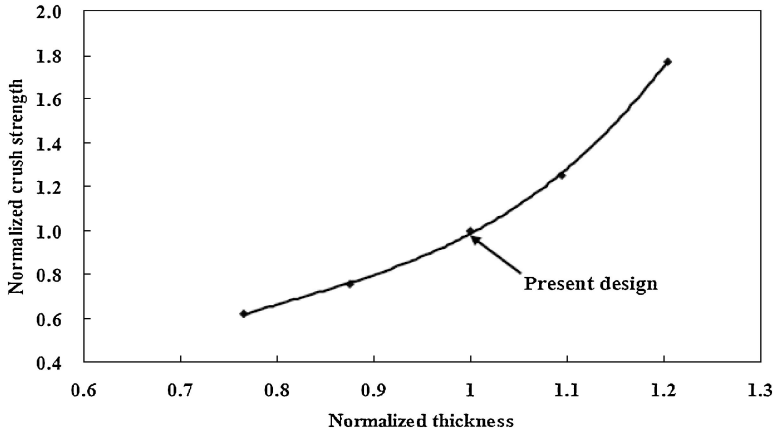

Fig. 10 Crush strength *vs.* strap thickness

Table 1 Normalized enhancement of a fuel rod support before and after optimization

Performance parameter	Before optimization	After optimization	
		Type A	Type B
Contact area	1.000	3.033	4.142
Peak stress	1.000	0.982	0.955
Plastic deformation	1.000	<0.50	<0.333

by a design optimization using homology constraints. Since it was known that the ligaments near the spring hardly affect the crush strength,[22] we only considered the spacer grid without ligaments (Type B in Fig. 9) near the spring in the next sections for the enhancement of the crush strength.

III. Enhancement of the Crush Strength of a Spacer Grid Assembly

1. Strap Thickness

A grid strap's thickness has generally been considered as one of the main design variables in order to regulate the crush strength of a spacer grid assembly, which is defined as the ability of resistance to lateral loads. **Figure 10** shows the relationship between a grid strap's thickness and crush strength, where the crush strength has a cubic relationship with a grid strap's thickness.[20] However, this design variable for a spacer grid assembly is very closely related with the pressure drop of a coolant; its application to a spacer grid design is significantly restrictive. Therefore, we did not consider this to be an effective measure for enhancing the crush strength of a spacer grid assembly.

2. Strap Height

A total grid strap's height has generally been considered as one of the main design variables in order to regulate crush strength. However, this design variable for a spacer grid assembly is also very closely related with the pressure drop of a coolant; its application to a spacer grid design is significantly restrictive. Therefore, we did not consider this to be an effective measure for enhancing the crush strength of a spacer grid assembly.

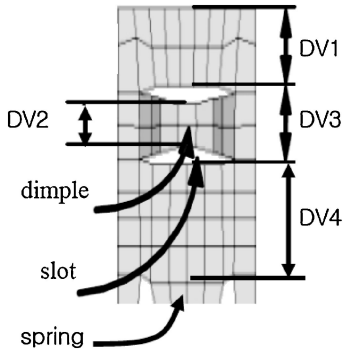

Fig. 11 Design variables for optimization of dimple location

3. Optimization of Dimple Location

Recently, it has been reported that dimple location is also a design variable that affects the crush strength of a spacer grid assembly. An effort to improve the crush strength of a spacer grid using an axiomatic design and optimization skills has been reported.[7] And the effect of dimple location in a spacer grid on crush strength has been investigated in a parametric study of the design variables in a spacer grid strap.[8] **Figure 11** shows the design variables for the optimization of dimple location, where the spring length and the total height of a grid strap maintain constant values, and the enhancement of crush strength of up to about 12.6% was obtained by the optimization of a dimple location from the analysis on subsized (7×7 type) specimens.[23] Thus, it could be very helpful for designing a spacer grid assembly if a new design variable is deduced without affecting so much the pressure drop of a coolant. Therefore, we did consider this to be an effective measure for enhancing the crush strength of a spacer grid assembly.

4. Increasing the Weld Line Length

The crush strength of a spacer grid assembly is strongly related to the buckling strength of the spacer grid straps

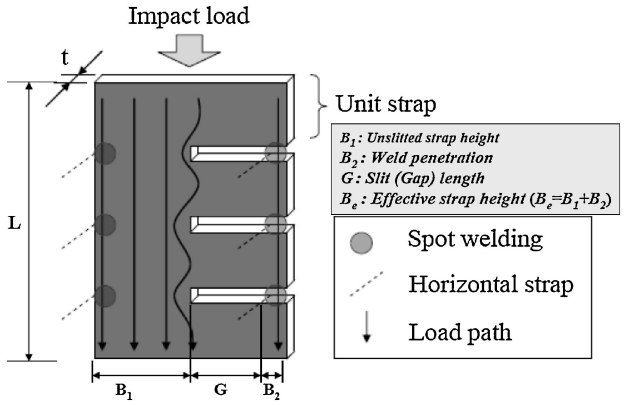

Fig. 12 Effective height for a grid strap

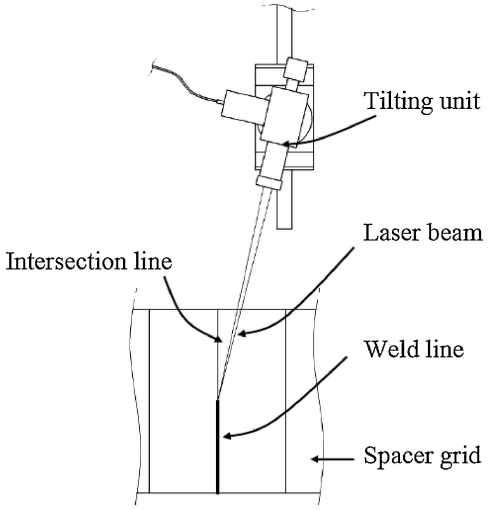

Fig. 13 Proposed LASER welding techniques (Tilting unit)

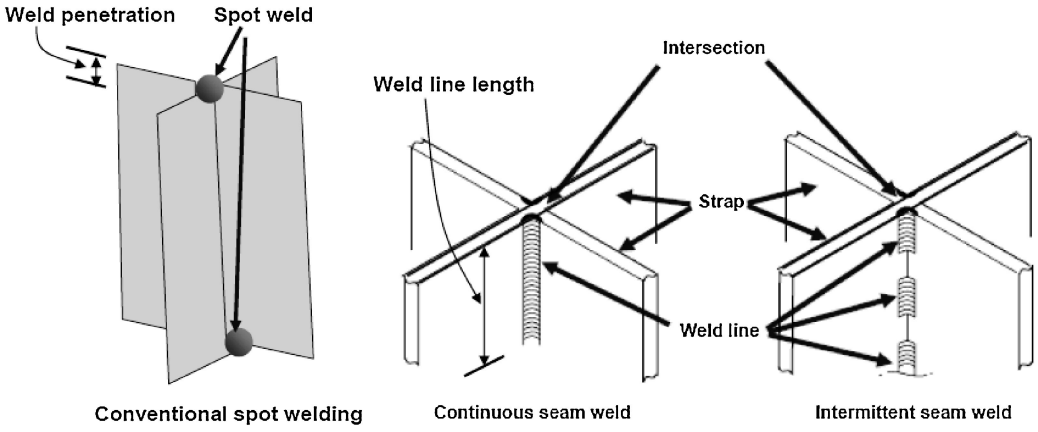

Fig. 14 Weld line for the proposed LASER welding techniques

constituting the spacer grid assembly. Based on the fact that the critical load (P_{cr}) is proportional to the moment of inertia (I), P_{cr} can be enlarged by increasing the plate thickness (t) and the effective height (B_e) of a strap as shown in **Fig. 12** and Eq. (8), where E and L refer to the elastic modulus and the length of strap, respectively. B_e refers to the part in a strap where a load passes, which is smaller than the height of a strap ($B_1 + G + B_2$).

$$P_{cr} \propto \frac{EI}{L^2} \propto B_e \bullet t^3 \tag{8}$$

Figure 12 shows a simple case where there are no dimples and springs, and we can improve P_{cr} by increasing B_e or reducing the slit (gap) length (G). Therefore, increasing the effective height, including the weld line length by maintaining the total height of the grid straps, could increase the buckling strength of the grid straps, and consequently, also the crush strength of the spacer grid assembly without increasing the pressure drop of a coolant.

Nowadays, laser beam welding (LBW) is prevalent for most of the Zircaloy spacer grid manufacturing vendors, for the purposes of smaller bead size and larger weld penetration at the welding parts. A spacer grid assembly with a smaller bead size leads to a smaller pressure drop of the coolant flowing along the fuel assembly, which consequently leads to a reduction in the load on a reactor coolant pump. In addition, a spacer grid assembly with a deeper weld penetration results in a larger crush strength of a spacer grid assembly, which is very important for the seismic resistance of a nuclear fuel assembly. However, a conventional laser spot welding with a high-energy input at the intersection points usually results in spattering and a larger bead size, which is a demerit for a spacer grid assembly performance in reactors. Hence, a seam welding method along an intersection between inner grid straps could be proposed as one of the alternatives to solve these demerits. We developed a new welding technique and a welding unit in the case of using the same LASER welder (Miyachi ML-2550A) for a conventional spot welding. The new LBW technique is constructed by tilting the LASER beam along the intersection line of the spacer grid assembly in order to obtain a longer weld line and a smaller weld bead size. Tilting the LASER beam is achieved by using the apparatus as shown in **Fig. 13**.[24] Weld lines for the new LASER welding technique are illustrated in **Fig. 14** in the case of a continuous seam weld and an intermittent seam weld.

IV. Crush Strength Analysis and Test

1. Crush Strength Test

A pendulum-type impact tester,[6] which is composed of a structural body, an impact hammer, a data acquisition system, and a furnace, was used to perform the impact test of the spacer grid assembly. The total moving mass of the impact tester is about 90 kg, which contains a hammer, connecting rods, and sensors for the crush strength test of a full-arrayed (16 × 16 type) spacer grid assembly. When the pendulum angles of the impact tester were increased, impact loads were measured at sensors. At a certain pendulum angle, some grid cells in the spacer grid assembly experienced a local buckling, and later, the measured impact load suddenly dropped. We define the impact load as crush strength. It is intended to simulate the type of load and impact velocities anticipated under a seismic disturbance.

2. FE Analysis

First of all, in order to check the validity of the FE model, the FE modeling of the 3 × 3 spacer grid assembly has been done by interconnecting the slotted grid straps and welding the intersections as shown in **Fig. 15**. The intersecting part is simply illustrated in Fig. 15(a), where the position of a spot welding is indicated as circles at both ends. In the FE model, six node solid elements are used to model the welding bead, which shares the nodes with the shell elements, and contact conditions are applied along the intersecting slots (the enlarged subfigures in Fig. 15(b)); the two intersecting straps at 90 degrees do not interfere with each other. In this FE model, S3R (3-node triangular general-purpose shell, finite membrane strains) and S4R (4-node doubly curved general-purpose shell, reduced integration with hourglass control, finite membrane strains) shell elements and C3D6 (6-node linear triangular prism) solid elements in ABAQUS[25] have been used: a total of 7,246 nodes and 6,070 elements. The FE analysis is carried out by considering a real impact experiment environment as follows. 1) An impact hammer is modeled as a rigid element with an equivalent mass. 2) The contact condition is applied between the rigid plate and the support grids. 3) The nodes at the bottom plate are fixed. The FE analysis model is shown in Fig. 15(c). The initial impact velocity at the reference node (at the center of the upper rigid surface) is applied, and the output accelerations for the initial impact velocity are obtained at this node. The impact force of the grid is evaluated by multiplying the maximum acceleration of the model by the mass of the impact hammer. The impact force generally increases as the velocity increases, but for a certain case, it decreases where the structure is considered to experience buckling. The critical impact load (crush strength) is taken as the impact force from this case where the peak point is observed.

Second, the FE models for the subsized (7 × 7 type) and the fully arrayed (16 × 16 type) spacer grid assembly for the impact analysis were also modeled. **Figures 16** and **17** show the FE models for the subsized and the fully arrayed spacer grid assembly, respectively. In the FE analysis model, a rigid and mass element was used for the impact hammer as shown in Figs. 16 and 17. All degrees of freedom were fixed at the rigid surface of the bottom side as shown in Figs. 16 and 17.

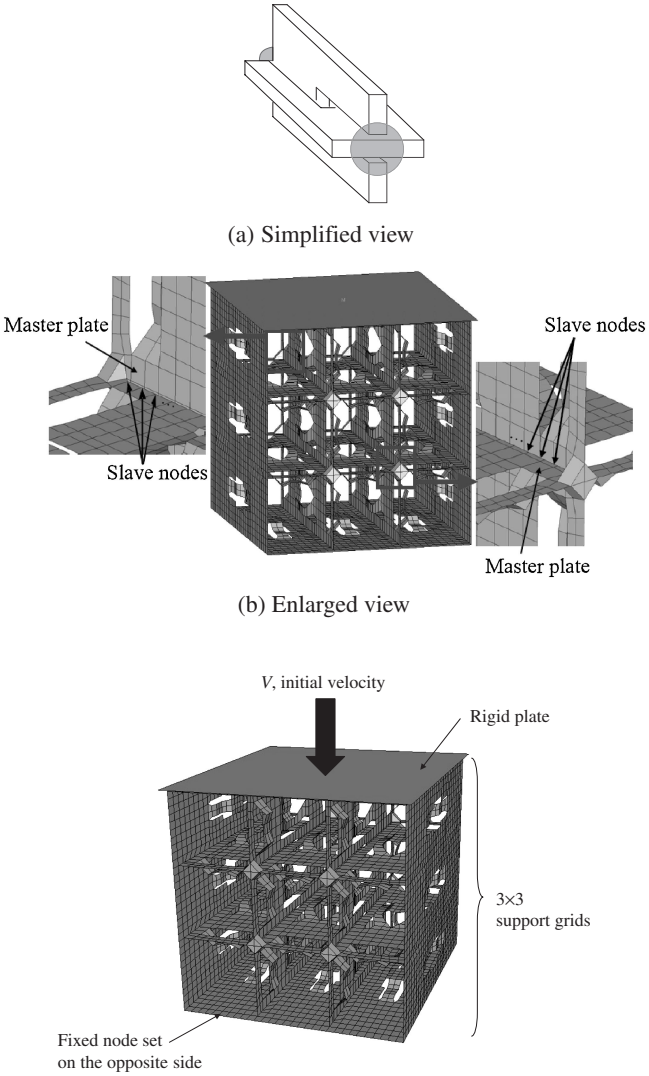

Fig. 15 Detailed view at an intersection

It is known that the welding penetration depth affects the crush strength of a spacer grid assembly to some extent.[7] Crush test and FE analysis for the subsized (7 × 7 type) spacer grid assembly shown in Fig. 16 were performed. **Table 2** shows the geometric data for the subsized specimen, and **Table 3** shows the test and analysis results for the subsized specimen. The test results were obtained from an average of 5 or 13 specimens. According to Table 3, the tendencies of a crush strength increase from the analysis are in good agreement with those from the test. The discrepancy between the test and the analysis results is attributed to the manufacturing dimensional tolerances and a local thinning of the strap thickness around the welded parts, whereas fixed dimensions were assumed in the analysis. We found that the crush strength was enhanced by up to 34% with an increase in the weld line length when compared with that of the conventional spot welding method for the 7 × 7 subsized spacer grid specimen.

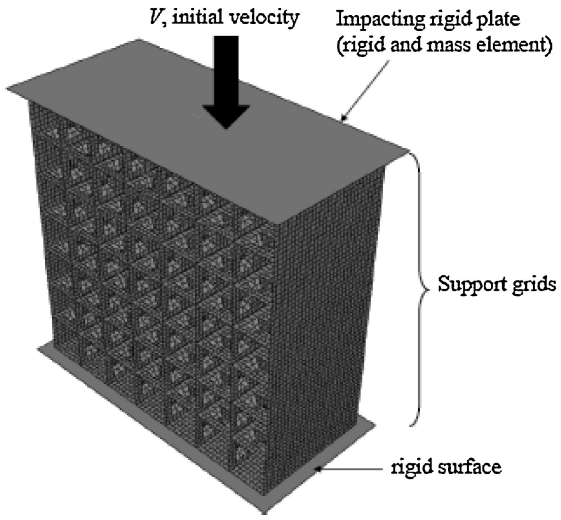

Fig. 16 Boundary and loading conditions for the subsized spacer grid assembly

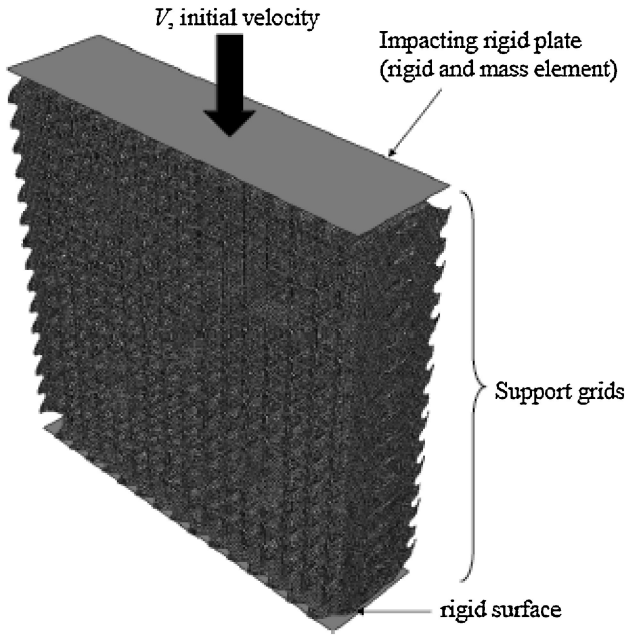

Fig. 17 Boundary and loading conditions for the full-arrayed spacer grid assembly

Figure 18 shows the normalized crush strength enhancement for the fully arrayed spacer grid assembly with guide tubes from the test and FE analysis with an increase in the normalized weld line length. The normalized weld line length is defined as a ratio of the actual weld line length by a continuous or intermittent seam weld to weld penetration by a conventional spot weld as shown in Fig. 14. The crush strength enhancement has a good linear relation with the weld line length as shown in Fig. 18 from the finite element analysis and test. According to Fig. 18, a considerable crush strength enhancement, *i.e.*, up to 60%, was achieved by the proposed welding method compared with that by the conventional spot welding method.

Table 2 Geometric data for the subsized (7 × 7 type) specimens

Specimen type	7 × 7
Cell pitch (mm)	12.7
Outer strap thickness (mm)	0.664
Inner strap thickness (mm)	0.457
Strap height (mm)	40.0

Table 3 Buckling strength increase ratio based on the value of a welding point at an intersection for the subsized specimen

Weld penetration (mm)	Analysis	Test	Remark
Point welding (2.0)	1.000	1.000	Conventional weld
9.275	1.145	1.154	
13.280	1.337	1.373	

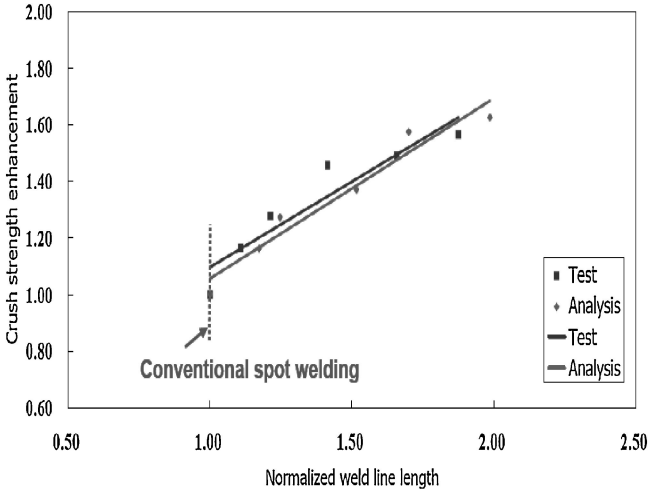

Fig. 18 Crush strength enhancement for the fully arrayed spacer grid assembly with guide tubes

V. Conclusions

A new spacer grid form and its manufacturing technology was suggested in order to enhance the integrity of a fuel rod support and the crush strength of a spacer grid assembly by using a systematic optimization technique without significantly increasing the pressure drop across the reactor core. The enhancement of the fuel rod support was confirmed by comparisons of the contact area, peak stresses, and plastic deformation, while the enhancement of the crush strength was investigated for both subsize support grids and a 16 × 16 full-size support grid. And the enhancement of the crush strength due to the increase in the weld line length was also investigated for a spacer grid assembly with the guide tubes from the test and FE analysis.

Acknowledgements

The work described in this paper was supported by the Small and Medium Business Administration (SBMA) of Korea.

References

1) H. J. Kunz, R. Schiffer, K. N. Song, *Fuel Assembly Mechanical Design Manual*, Siemens/KWU Work-Report U6 312/87/e326 (1987).
2) L. A. Walton, "Zircaloy spacer grid design," *Trans. Am. Nucl. Soc.*, **32**, 601–602 (1979).
3) J. G. Larson, "Optimization of the Zircaloy space grid design," *Trans. Am. Nucl. Soc.*, **43**, 160–161 (1982).
4) K. H. Yoon *et al.*, "Shape optimization of the H-shape spacer grid spring structure," *J. Korean Nucl. Soc.*, **33**[5], 547–555 (2001).
5) K. N. Song *et al.*, "Shape optimization of a nuclear fuel rod support structure," *Proc. 16th Int. Conf. on Structural Mechanics in Reactor Technology*, Washington, DC, USA, Aug. 12–17, 2001 (2001), [CD-ROM].
6) K. H. Yoon *et al.*, "Dynamic impact analysis of the grid structure using multi-point constraint (MPC) equation under the lateral impact load," *Computers & Structures*, **82**[23–26], 2221–2228 (2004).
7) S. H. Lee *et al.*, "Design improvement of an OPT-H type nuclear fuel rod support grid by using an axiomatic design and an optimization," *J. Mech. Sci. Technol.*, **21**, 1191–1195 (2007).
8) S. B. Lee *et al.*, "Parametric study of a dimple location in a spacer grid under a critical impact load," *J. Mech. Sci. Technol.*, **22**, 2024–2029 (2008).
9) J. K. Kim, *Shape Optimization of a Nuclear Fuel Rod Spacer Grid Considering Impact and Wear*, Master thesis, Hanyang University, Korea (2007).
10) M. K. Shin *et al.*, "Optimization of a nuclear fuel spacer grid spring using homology constraints," *Proc. 15th Int. Conf. on Nuclear Engineering*, Nagoya, Japan, Apr. 22–26, 2007, ICONE 15-10366 (2007), [CD-ROM].
11) K. H. Lee *et al.*, "Truss optimization considering homologous deformation under multiple loadings," *Structural Optimization*, **16**[2–3], 193–200 (1998).
12) K. H. Lee, G. J. Park, "Structural homology design using equality constraints for linear and nonlinear conditions," *Int. J. Jpn. Soc. Mech. Engineers, Series C*, **40**[1], 150–156 (1997).
13) S. V. Hoerner, "Homologous deformation of tilt table telescopes," *J. Structural Division, ACSE*, **93**, 461–485 (1967).
14) S. Nakagiri *et al.*, "A note on finite element synthesis of structures (part 7), Formulation of homologous vibration mode," *Seisan Kenkyu*, **44**[9], 449–452 (1992).
15) J. W. Ha *et al.*, "Experimental analysis on the influences of support condition and shape in fuel fretting wear," *Proc. Korea Nuclear Society Fall Annu. Mtg.*, Yongpeong, Kangwondo, Korea, Oct. 24–25, 2002 (2002), [CD-ROM].
16) M. W. Kennard *et al.*, *A Study of Grid-to-Rod Fretting Wear in PWR Fuel Assemblies*, Vol. 1, S. M. Stoller Co., Broomfield (1995).
17) Y. H. Lee *et al.*, "Effects of contact shape and environment in fuel fretting wear," *Proc. Korea Nuclear Society Fall Annu. Mtg.*, Yongpeong, Kangwondo, Korea, Oct. 24–25, 2002 (2002), [CD-ROM].
18) M. K. Shin *et al.*, "Optimization of a nuclear fuel spacer grid spring using homology constraints," *Nucl. Eng. Des.*, **238**, 2624–2634 (2008).
19) K. N. Song *et al.*, "Development of a new spacer grid form to enhance the integrity of fuel rod support and the crush strength of a spacer grid assembly," *Proc. 17th Int. Conf. on Nuclear Engineering*, Brussels, Belgium, Jul. 12–16, 2009, ICONE 17-75008 (2009), [CD-ROM].
20) K. N. Song *et al.*, "Design of a nuclear fuel rod support grid using axiomatic design," *Trans. Korea Soc. Mech. Eng. A*, **26**[8], 1623–1630 (2002), [in Korean].
21) *GENESIS User's Manual*, Version 7.5, Vanderplaats Research and Development Inc., Colorado Springs (2004).
22) G. J. Park, J. J. Lee, K. N. Song, *Topology Design and Manufacturing of a Grid Strap to Enhance the Impact Strength of a Grid Assembly*, KAERI/CM-1079/2008 (2008), [in Korean].
23) K. N. Song *et al.*, "Development of a new spacer grid form to enhance the integrity of fuel rod support and the crush strength of a spacer grid assembly," *2008 Water Reactor Fuel Performance Mtg.*, Seoul, Korea, Oct. 19–23, 2008, WRFPM2008-8115 (2008), [CD-ROM].
24) K. N. Song, S. S. Kim, "Laser welding unit for intersection line welding of spacer grid inner straps and its application," *J. Laser Micro/Nanoengineering*, **4**[1], 11–17 (2009).
25) *ABAQUS Analysis User's Manual*, Version 6.7 (2007).